Electronic Supplementary Material (ESI) for Journal of Materials Chemistry C.

SUPPORTING INFORMATION:

Charge Transport in Nanoparticular Thin Films of Zinc Oxide and Aluminum-doped Zinc Oxide

Thomas Lenz, Moses Richter, Gebhard J. Matt, Norman A. Luechinger, Samuel C. Halim, Wolfgang Heiss, and Christoph J. Brabec

Further experimental details:

Substrates with ITO on glass were received from Weidner Glas GmbH. Structuring of the back contacts was achieved by laser ablation. The substrates were cleaned in ultrasonic bath of both acetone and 2-propanol each for at least 10 minutes. Then, the nanoparticular dispersions were deposited onto the substrate via doctor blading. In order to achieve film thicknesses in the range of 1 µm, the blading step was repeated several times each time followed by short annealing at 80°C for one minute. Final annealing was at 80°C for 10 minutes. The annealing as well as the blading were performed under ambient condition in a Class ISO 3 clean-room. Film thicknesses were measured with a KLA Tencor D-100 and were 740 ± 21 nm and 950 ± 28 nm for ZnO and AZO, respectively. Silver as top contact (~100 nm) was thermally evaporated through shadow masks in vacuum ($8 \cdot 10^{-6}$ mbar) with a deposition rate of 0.5 – 3 Å/s. The resulting device cross section was 0.1 cm^2.

The samples were electrically characterized in a N_2-cryostat using a Keithley 236 Source Measurement Unit in the temperature range of 170 – 300 K (steps of 10 K).

The high resolution transmission electron microscopy phase contrast images were obtained with a JEOL 2011 FasTEM transmission electron microscope, operated at an acceleration volt age of 200 kV.

Additional results and Figures

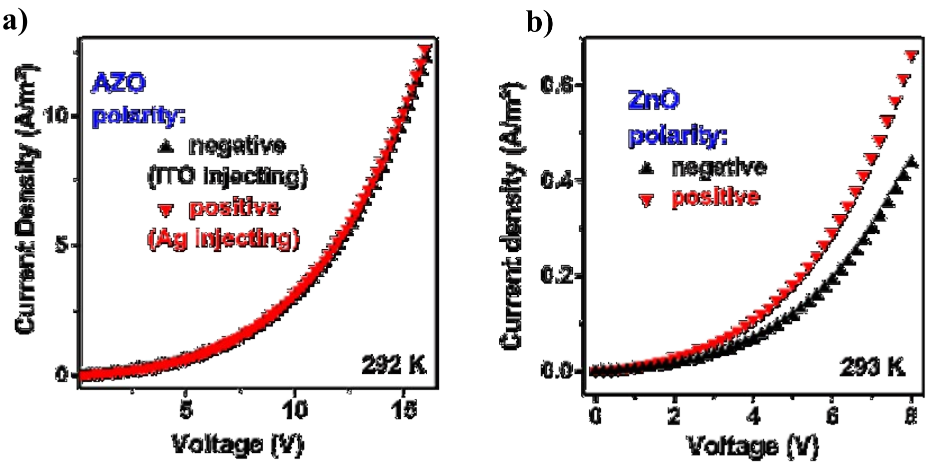

Figure S1: a) Current density-voltage (J-V) characteristic of AZO at 292 K for positive and negative polarity. For the latter, the absolute value of current density was plotted versus the absolute value of voltage, so that a comparison of the two polarities is possible. The two curves lie on one another confirming the symmetry of the characteristic.

b) Current density-voltage (J-V) characteristic of ZnO at 293 K for positive and negative polarity. The symmetry for ZnO is a bit worse compared to AZO, electron injection from Ag works a bit more efficient than electron injection from ITO. But the general curve progression is very similar for both. This confirms the bulk-limited charge transport character, as it is the case for AZO.

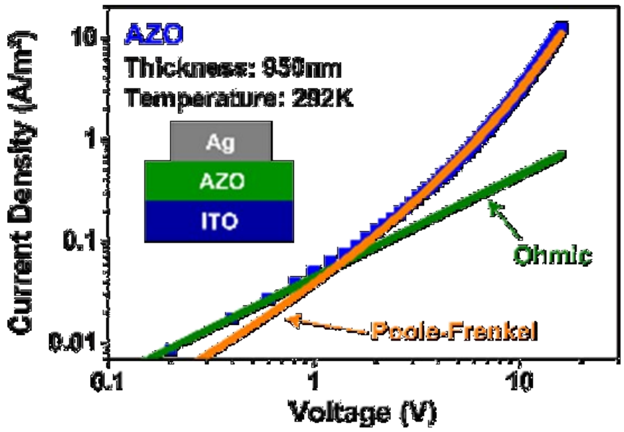

Figure S2: a) J-V characteristics of AZO in a double-logarithmic plot. Two fit functions demonstrate that the low voltage data is nicely described by Ohmic behavior, while the high voltage data follows Poole-Frenkel effect. This could be further demonstrated when plotting the data according to Equation 3 (see Manuscript).

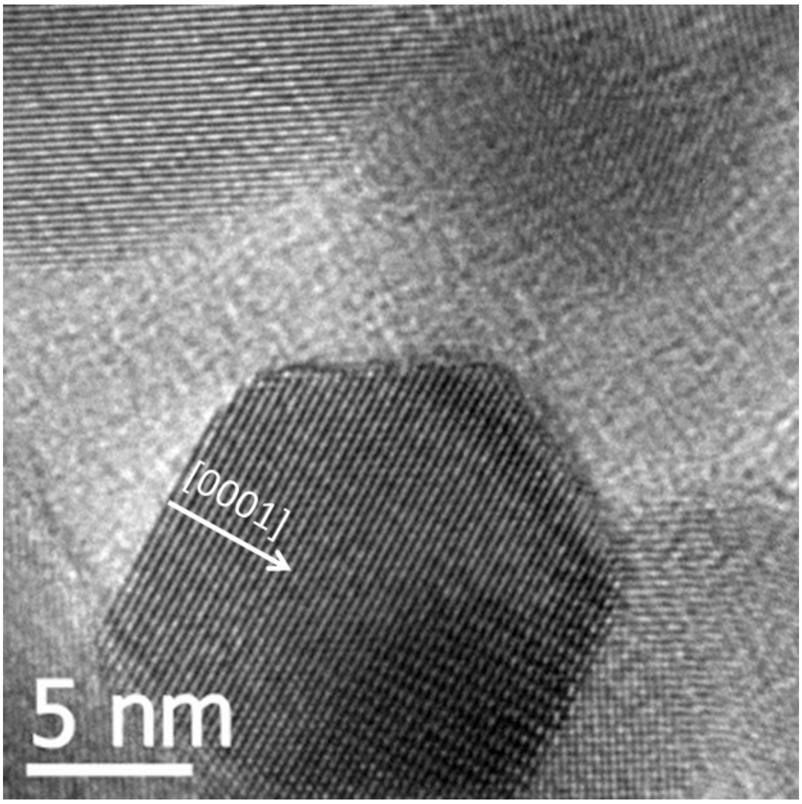

Figure S3: TEM picture of the AZO nanoparticles. As additional information we inserted the [0001] orientation into the picture. The spacing here is roughly 0.28 nm/fringe.

Table S1: Slopes and y-intercepts of the linear regimes in the Poole-Frenkel plot of AZO and the resulting experimental values of β.

AZO (950 nm)			
Temperature [K]	**Slope [$m^{0.5}$ $V^{-0.5}$]**	**β [$eVm^{0.5}V^{-0.5}$]**	**ln σ_0**
194	0.00135	$2.25 \cdot 10^{-5}$	-25.69803
200	0.00131	$2.25 \cdot 10^{-5}$	-25.37809
212	0.00127	$2.32 \cdot 10^{-5}$	-25.06758
223	0.00123	$2.36 \cdot 10^{-5}$	-24.76875
234	0.00119	$2.40 \cdot 10^{-5}$	-24.47576
245	0.00116	$2.45 \cdot 10^{-5}$	-24.1819
251	0.00114	$2.47 \cdot 10^{-5}$	-24.01716
263	0.0011	$2.49 \cdot 10^{-5}$	-23.69447
274	0.00107	$2.53 \cdot 10^{-5}$	-23.41668
285	0.00104	$2.55 \cdot 10^{-5}$	-23.09004
298	0.001	$2.56 \cdot 10^{-5}$	-22.78357

Table S2: Slopes and y-intercepts of the linear regimes in the Poole-Frenkel plot of ZnO and the resulting experimental values of β.

ZnO (740 nm)			
Temperature [K]	**Slope [$m^{0.5}$ $V^{-0.5}$]**	**β [eV$m^{0.5}V^{-0.5}$]**	**ln σ_0**
189	0.00168	$2.74\cdot10^{-5}$	-31.37495
200	0.00154	$2.65\cdot10^{-5}$	-30.39842
211	0.00146	$2.65\cdot10^{-5}$	-29.58766
222	0.00139	$2.66\cdot10^{-5}$	-28.78824
232	0.00132	$2.64\cdot10^{-5}$	-27.9833
242	0.00125	$2.61\cdot10^{-5}$	-27.15632
253	0.00119	$2.59\cdot10^{-5}$	-26.35663
263	0.00113	$2.56\cdot10^{-5}$	-25.61871
273	0.0011	$2.59\cdot10^{-5}$	-24.98272
283	0.00108	$2.63\cdot10^{-5}$	-24.54576
293	0.00109	$2.75\cdot10^{-5}$	-24.54866